



**LIGHTWEIGHT STRUCTURES in CIVIL ENGINEERING  
CONTEMPORARY PROBLEMS**

Monograph from Scientific Seminar  
Organized by Polish Chapters of  
**International Association for Shell and Spatial Structures**

Łódź University of Technology  
Faculty of Civil Engineering, Architecture  
and Environmental Engineering

**XXVII LSCE**  
**Łódź, 2<sup>nd</sup> – 3<sup>rd</sup> of December 2021**



**MODERN SOLUTION OF TUBE TELECOMMUNICATION TOWER –  
PROBLEMS, ANALYSIS AND PERSPECTIVES**

**J. Szafran**<sup>1)</sup> **K. Juszczak-Andraszyk**<sup>2)</sup>

<sup>1)</sup> BEng, PhD, DSc, Faculty of Civil Engineering, Architecture and Environmental Engineering,  
Lodz University of Technology, POLAND, [jacek.szafran@p.lodz.pl](mailto:jacek.szafran@p.lodz.pl)

<sup>2)</sup> PhD, Compact-Project Company, POLAND, [kjuszczak-andraszyk@compact-project.pl](mailto:kjuszczak-andraszyk@compact-project.pl)

**ABSTRACT:** The paper emphasizes aspects that have to be addressed when analyzing monopole structures, such as vortex excitation occurring due to a repeating pattern of vortex shedding in the flow of air around a tower (von Kármán vortex street). The fatigue analysis is discussed in detail in the paper and it presents solutions that were introduced on the basis of the analysis results in order to reinforce certain areas of the tower (stress concentration in the vicinity of structural details required due to technological reasons).

**Keywords:** monopole tower, telecommunication tower, vortex excitation, fatigue analysis, 5G network.

## 1. INTRODUCTION

It is difficult to imagine today's world without high-speed data transmission capabilities at any distance. Billions of Earth's inhabitants use devices designed to make phone calls and send text and graphic messages on a daily basis. As technologies used in mobile devices are advancing, including smartphones and tablets that replace computers in a number of applications, users demand wireless, high-speed and reliable Internet access as standard.

Today we can see the fifth generation networks (5G) grow with increasing number of devices connected to them. Internet of Things (IoT) is a concept of material objects connected with each other and with Internet resources via a powerful computer network, i.e. the Internet. The main goal of the IoT is the creation of smart areas such as smart cities, transport, products, buildings, power systems, health systems or systems related to everyday life. Such a smart area can be developed provided that technologies necessary to implement it have been delivered. Data exchange between all users sets increasingly higher requirements on networks and their operators. The 5G standard is meant to meet these expectations by providing faster Internet connections and enabling many devices to communicate concurrently. One of requirements that have to be satisfied in order for 5G to be properly implemented and operated is building new base stations, and the Polish Ministry of Digital Affairs expects their total number to be 10 to 100 times bigger than in 3G or 4G networks. These new base stations are being built both in open suburban and rural areas and in city centers. A wide diversity of support structures erected for telecommunications purposes can be found around the world (Smith 2007). The choice of a structure to serve as a support for telecommunications equipment is mostly based on purely technical requirements, but aesthetic reasons are also becoming important particularly for structures located in urban areas. What is essential is that these objects should not stand out

nor require much space and should be relatively fast and simple to build compared to traditional solutions. At the same time the structures need to be safe and durable.

The paper proposes a comprehensive structural solution of a monopole telecommunications tower that ideally meets the above mentioned requirements. Technological solutions and the structural analysis are discussed including issues that were encountered and ways in which these were solved.

## 2. TOWER STRUCTURE

The structure under consideration is a steel tower solid-wall pole measuring 30.0 m in height (32.53 m including the spire). The structure is made of 4 segments with the three bottom ones having the cross-section in the shape of a regular octadecagon, and the upper one made of a circular hollow section. The middle segments (S-2 and S-3) have a taper and are joined to each other by means of a slip joint connection (a telescopic connection) with an overlap of about 1.5 m. The other segments and the core of the tower with the foundation are joined to each other by means of flanged bolted connections. The entire structure has been designed of S355 steel grade. Table 1 summarizes basic characteristics of the tower segments.

Table 1. Basic characteristics of the tower segments.

| Segment   | Segment height [m] | Cross sections of core members / wall thickness [mm] | Lower circumcircle/<br>incircle diameter [m] | Wall thickness [mm] |
|-----------|--------------------|--|--|---------------------|
|           |                    |  | Upper circumcircle/<br>incircle diameter [m] |                     |
| S-1 (top) | 7.700              | RO 245x12  | -  | -                   |
| S-2       | 8.044              | Regular octadecagon / 5.0                            | 0.971/ 0.956<br>0.711/ 0.700                 | 5.0                 |
| S-3       | 8.000              | Regular octadecagon / 6.0                            | 1.170/ 1.152<br>0.911/ 0.897                 | 6.0                 |
| S-4       | 7.800              | Regular octadecagon / 6.0                            | 1.170/ 1.152<br>1.170/ 1.152                 | 6.0                 |

Inside the lowest segment of the tower, there is a system of support structures used to mount telecommunication devices serving the BTS. Four ventilated doors are provided to access the equipment in the member. Additional system members (anchoring devices), designed to provide the telescopic connection, are mounted on segments S-2 and S-3.

Support structures (frames and anchoring devices) are mounted on the circular section of segment S-1; by means of these structures, sector antennas (3 pieces) and RRUs are mounted. An antenna beautification cover is provided around the segment along its full height, made of two parts: the lower one 3.74 m in height and the upper one 3.79 m in height, both 1.35 m in their outer diameter.

On the tower top, there is a spire made of circular hollow sections Ø76 mm, Ø60 mm and Ø42 mm, to which a support structure (a frame) for mounting microwave antennas is fixed. The spire is mounted by means of a flanged connection. The view of tower structure is presented on Fig. 1.

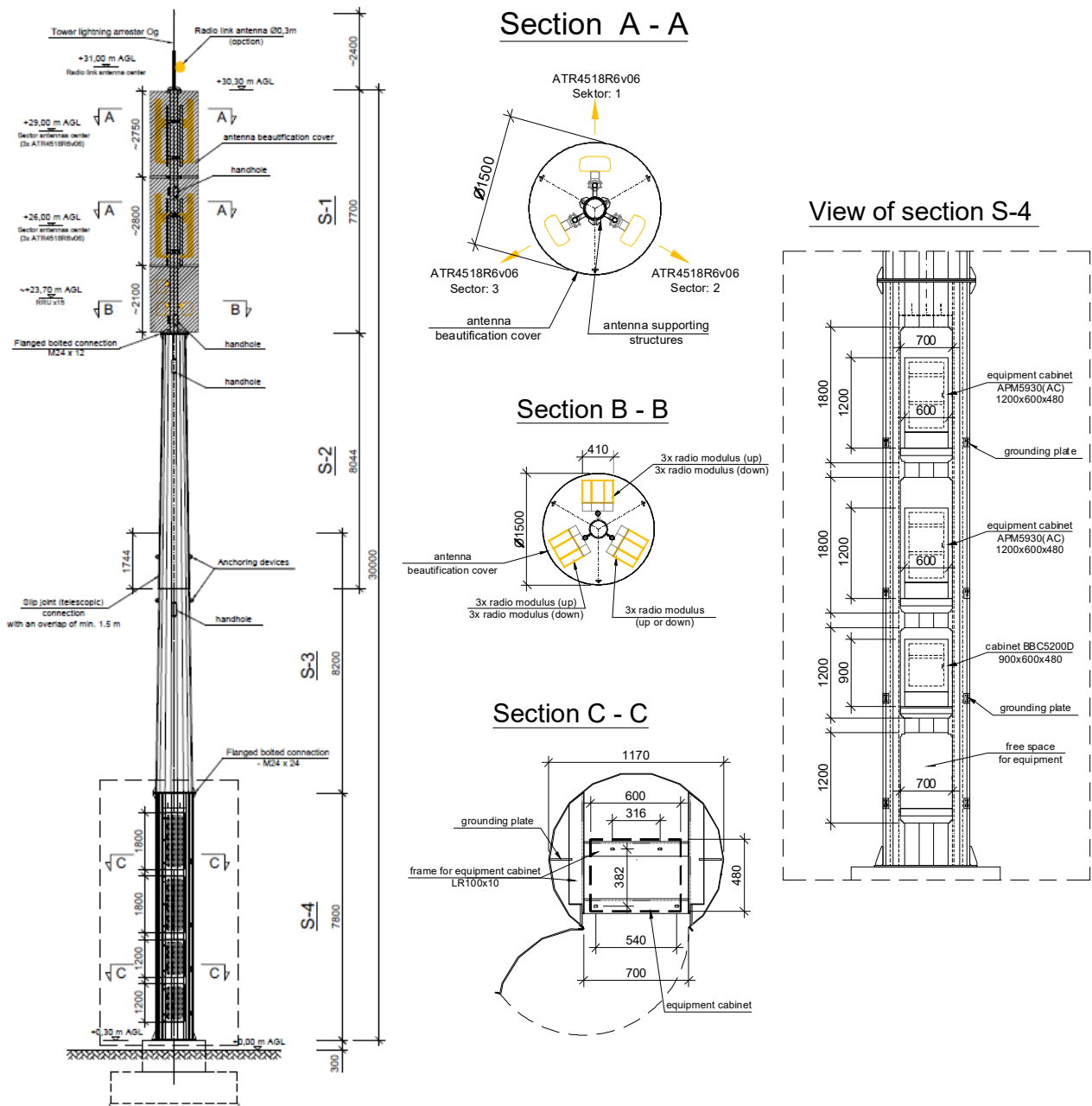


Fig. 1 The view of tower structure, dimensions in mm.

### 3. STRUCTURAL ANALYSIS

#### 3.1. Alongwind load effects

It was assumed that the structure would be located in wind load zone 1, for which the basic wind velocity pressure is  $q_b = 0.3 \text{ kN/m}^2$ , in a terrain corresponding to terrain category II (areas with low vegetation, such as grass, and single obstacles, such as trees and buildings, not less than 20 times their height apart).

Wind load on the tower core was calculated according to PN-EN 1991-1-4. Due to the central symmetry of the core structure cross-section, a single wind load direction was considered in calculations.

The mean wind load on the tower in the wind direction was calculated with the following formula:

$$F_w = c_s c_d \cdot c_f \cdot q_p(z_e) \cdot A_{ref}, \quad (3.1)$$

where  $c_s c_d$  is structural factor,  $c_f$  is total wind force coefficient (for the aerodynamic drag),  $q_p(z_e)$  refers to peak velocity pressure and  $A_{ref}$  describes reference area.

The aerodynamic drag factor for segments S-2, S-3, and S-4 was determined as for regular polygons (octadecagons) and for segment S-1 as for circular cylinders, whereby geometrical data of a segment cover were taken in calculations.

The structural factor was determined using the following formula:

$$c_s c_d = \frac{1 + 2 \cdot k_p \cdot I_v(z_s) \cdot \sqrt{B^2 + R^2}}{1 + 7 \cdot I_v(z_s)}, \quad (3.2)$$

where  $k_p$  refers to peak factor defined as the ratio of the maximum value of the fluctuating part of the response to its standard deviation,  $I_v$  is turbulence intensity,  $z_s$  describes reference height for calculating the structural factor,  $B^2$  is out-of-resonance response factor, allowing for the lack of full correlation of the pressure on the span, and  $R^2$  is resonance response factor, allowing for turbulence in resonance with the vibration mode of the structure.

Wind actions on equipment and support structures were calculated in the same way as the wind force on the tower core, each time considering the height where a given device, or a support structure is mounted.

Aerodynamic drag coefficients for the support structures were calculated as for the core structure dividing structural members into those with sharp edges and those in the shape of a circular cylinder.

The aerodynamic drag coefficient for the telecommunication equipment (the microwave antenna) was taken as  $c_f = 1.2$ .

### 3.2. Crosswind action

In addition to the response of the structure to wind loading parallel to wind direction, possible occurrence of vortex excitation, resulting in load fluctuations in the plane perpendicular to wind direction should be considered for structures with a solid-wall circular cross-section. This phenomenon occurs when vortices are shedding in turn from the opposite sides of a structure. Vibrations of the structure can occur if the frequency of vortex shedding matches the eigenfrequency of the structure. This condition is satisfied if wind velocity equals critical wind velocity given by the formula:

$$v_{crit,i} = \frac{b \cdot n_{1,y}}{St}, \quad (3.3)$$

where  $St$  is Strouhal number, for circular cross-sections equal to  $t = 0.18$ ,  $b$  is a cross-section diameter of a member and  $n_{1,y}$  is eigenfrequency of the structure, for towers defined as:

$$n_1 = \frac{46}{h} \text{ Hz}. \quad (3.4)$$

Vortex excitation should be considered if the ratio of the largest and the smallest measure of a structure in the plane perpendicular to the wind direction is greater than 6; in this case:

$$\frac{h}{b_{min}} = \frac{30.0m}{0.711m} = 49.2. \quad (3.5)$$

Vortex excitation does not have to be taken into account if:

$$v_{crit,i} > 1.25 \cdot v_m . \quad (3.6)$$

In this case:

$$v_{crit,i} = 11.5 \frac{m}{s} < 1.25 \cdot 26.5 \frac{m}{s} = 33.1 \frac{m}{s} . \quad (3.7)$$

Considering the above, the possible occurrence of vortex excitation should be taken into account for the structure in question.

The effect of vibrations induced by vortex excitation should be calculated based on inertial forces per unit length, exerted in the plane perpendicular to the wind direction at point  $s$ , according to the formula:

$$F_w(s) = m_e(s) \cdot (2 \cdot \pi \cdot n_{1,y})^2 \cdot \Phi_{i,y}(s) \cdot y_{F,max} , \quad (3.8)$$

where  $\Phi_{i,y}(s)$  is the natural mode shape of the structure normalized to unity at the point of maximum displacement,  $y_{F,max}$  is maximum displacement with time of the point at which  $\Phi_{i,y}(s)$  equals 1.

Approach 1 (according to PN-EN 1991-1-4, Annex E) was used to determine the amplitude of vibration in the plane perpendicular to the wind direction:

$$\frac{y_{F,max}}{b} = \frac{1}{St^2} \cdot \frac{1}{Sc} \cdot K \cdot K_w \cdot c_{lat} , \quad (3.9)$$

where  $Sc$  is Scruton number, equal to:

$$Sc = \frac{2 \cdot \delta_s \cdot m_e}{\rho \cdot b^2} , \quad (3.10)$$

$K$  is mode shape factor equal to  $K = 0.13$  for cantilevered structures,  $K_w$  refers to effective correlation length factor, for cantilevered structures given by the relation:

$$K_w = 3 \cdot \frac{L_1/b}{\lambda} \cdot \left[ 1 - \frac{L_1/b}{\lambda} + \frac{1}{3} \cdot \left( \frac{L_1/b}{\lambda} \right)^2 \right] , K_w \leq 0.6 , \quad (3.11)$$

$L_1$  is correlation length for the first mode shape,  $c_{lat}$  describe lateral load factor, related to the Reynolds number, for the case considered equal to  $c_{lat} = 0.2$ .

The amplitude of vibration and the correlation length were determined by means of the iterative method.

The number of loading cycles imposed by vortex-induced vibrations was calculated from the expression:

$$N = 2 \cdot T \cdot n_{1,y} \cdot \varepsilon_0 \cdot \left( \frac{v_{crit}}{v_0} \right)^2 \cdot \exp \left( - \left( \frac{v_{crit}}{v_0} \right)^2 \right) , \quad (3.12)$$

where  $T$  is design working life of the structure in seconds,  $\varepsilon_0$  is bandwidth factor allowing for the range of wind velocities causing vortex-induced vibrations; taken as equal to  $\varepsilon_0 = 0.3$ ,  $v_0$  refers to the modal value of the Weibull probability distribution assumed for the wind velocity in [m/s], multiplied by  $\sqrt{2}$ , equal to:

$$v_0 = 0.2 \cdot v_m . \quad (3.13)$$

### 3.3. Calculation model

The support structure was modeled using the Autodesk Robot Structural Analysis 2014 software, utilizing the finite element method, as a solid section structure and a shell structure. Six-degree-of-freedom (6DOF) solid section finite elements and triangular and quadrilateral shell finite elements were used. A support fixed in foundations was taken as the structural arrangement in both models.

Wind loads imposed on members were modeled as evenly distributed linear forces, while the load caused by antennas and supports as concentrated forces. In the shell structure model, wind loads were modeled as the surface loading per unit area.

The fatigue analysis was performed based on the calculation model developed in the Consteel 12 software as a shell structure. Shell finite elements in the shape of a triangle of side 100 mm on average were used.

Joints were analyzed with the aid of the IDEA StatiCa 9 software using the finite element method. Internal forces in each member were replaced with the load of a node in a local arrangement of connected rods.

### 3.4. Analysis of load-carrying capacity

The load-carrying capacity of the support structure for telecommunication equipment was determined according to PN-EN 50341.

Members were considered as solid-wall shell-type poles with a thin-wall cross-section in the shape of an octadecagonal hollow section for which the criterion of limit slenderness for the class 4 cross-section is:

$$\frac{b}{t} > 42\varepsilon, \quad (3.14)$$

where  $b$  and  $t$  are wall length and thickness respectively,  $\varepsilon = \text{square root of } 235/f_y$ , and  $f_y$  is the nominal value of the yield strength in  $\text{N/mm}^2$ .

The characteristics of polygonal cross-sections were calculated from the formulas:

- area:

$$A = (d - t) \sin\left(\frac{\pi}{n_k}\right) n_k t, \quad (3.15)$$

- moment of inertia:

$$I = \frac{n_k}{192} \tan\left(\frac{\pi}{n_k}\right) \left(3 + \tan\left(\frac{\pi}{n_k}\right)^2\right) (d_f^4 - (d_f - 2t)^4), \quad (3.16)$$

- elastic section modulus:

$$W_{el} = \frac{I}{\frac{d - t}{2}}, \quad (3.17)$$

where  $d$  describes outside diameter across angles of the polygon,  $n_k$  refers to number of sides and  $d_f$  is diameter at the crown, equals to:

$$d_f = d \cos\left(\frac{\pi}{n_k}\right). \quad (3.18)$$

The load-carrying capacity of class 3 polygonal cross-sections, without openings, will be satisfactory if the following condition is met:

$$\frac{N_{Ed}}{A} + \frac{M_{Ed}}{W_{el}} \leq \frac{f_y}{\gamma_{M1}}. \quad (3.19)$$

where  $N_{Ed}$  and  $M_{Ed}$  are design normal force and bending moment,  $A$  and  $W_{el}$  are gross cross-section area and elastic section modulus, and  $\gamma_{M1}$  is partial factor for resistance, for S355 steel equal to 1.15.

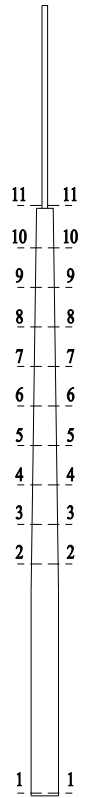
Tables 2 and 3 below include characteristics of cross-sections, design forces, and verification of the condition of load-carrying capacity at 11 points of the tower.

Table 2. Characteristics and effort of cross-sections 1 to 6.

| Cross section                               |               | 1        | 2        | 3        | 4        | 5        | 6        |
|---|---------------|----------|----------|----------|----------|----------|----------|
| Diameter, [mm]                              | $d$           | 1170     | 1138     | 1091     | 1043     | 996      | 948      |
| Thickness, [mm]                             | $t$           | 6        | 6        | 6        | 6        | 6        | 6        |
| Wall length, [mm]                           | $b$           | 203.2    | 197.6    | 189.5    | 181.1    | 173.0    | 164.6    |
| Number of sides, [-]                        | $n_k$         | 18       | 18       | 18       | 18       | 18       | 18       |
| Diameter at the crown, [mm]                 | $d_f$         | 1152.2   | 1120.7   | 1074.4   | 1027.2   | 980.9    | 933.6    |
| Gross cross-section, [cm <sup>2</sup> ]     | $A$           | 218.3    | 212.3    | 203.5    | 194.5    | 185.7    | 176.7    |
| Moment of inertia, [cm <sup>4</sup> ]       | $I$           | 362128.8 | 333074.3 | 293283.5 | 256053.5 | 222790.2 | 191928.1 |
| Elastic section modulus, [cm <sup>3</sup> ] | $W_{el}$      | 6222.1   | 5884.7   | 5406.1   | 4938.4   | 4500.8   | 4074.9   |
| Yield strength, [MPa]                       | $f_y$         | 355      | 355      | 355      | 355      | 355      | 355      |
| Epsilon, [-]                                | $\varepsilon$ | 0.814    | 0.814    | 0.814    | 0.814    | 0.814    | 0.814    |
| Cross section class check                   |               | 3 class  | 3 class  | 3 class  | 3 class  | 3 class  | 3 class  |
| Normal force, [kN]                          | $N_{Ed}$      | 74.02    | 57.77    | 55.13    | 52.6     | 50.19    | 47.88    |
| Bending moment, [kNm]                       | $M_{Ed}$      | 420.31   | 222.49   | 194.81   | 169.03   | 145.13   | 123.07   |
| $N_{Ed}/A + M_{Ed}/W_{el}$ , [MPa]          |               | 70.94    | 40.53    | 38.74    | 36.93    | 34.95    | 32.91    |
| $f_y/\gamma_{M1}$ , [MPa]                   |               | 308.70   | 308.70   | 308.70   | 308.70   | 308.70   | 308.70   |
| Cross-section effort, [%]                   |               | 23.0%    | 13.1%    | 12.6%    | 12.0%    | 11.3%    | 10.7%    |

Table 3. Characteristics and effort of cross-sections 7 to 11.

| Cross section                               |               | 7        | 8        | 9       | 10      | 11      |
|---|---------------|----------|----------|---------|---------|---------|
| Diameter, [mm]                              | $d$           | 901      | 853      | 806     | 758     | 245     |
| Thickness, [mm]                             | $t$           | 5        | 5        | 5       | 5       | 12      |
| Wall length, [mm]                           | $b$           | 156.5    | 148.1    | 140.0   | 131.6   | 42.5    |
| Number of sides, [-]                        | $n_k$         | 18       | 18       | 18      | 18      | 18      |
| Diameter at the crown, [mm]                 | $d_f$         | 887.3    | 840.0    | 793.8   | 746.5   | 241.3   |
| Gross cross-section, [cm <sup>2</sup> ]     | $A$           | 140.0    | 132.5    | 125.2   | 117.7   | 87.4    |
| Moment of inertia, [cm <sup>4</sup> ]       | $I$           | 137638.6 | 116680.7 | 98334.1 | 81693.2 | 5812.3  |
| Elastic section modulus, [cm <sup>3</sup> ] | $W_{el}$      | 3072.3   | 2751.9   | 2455.3  | 2169.8  | 498.9   |
| Yield strength, [MPa]                       | $f_y$         | 355      | 355      | 355     | 355     | 355     |
| Epsilon, [-]                                | $\varepsilon$ | 0.814    | 0.814    | 0.814   | 0.814   | 0.814   |
| Cross section class check                   |               | 3 class  | 3 class  | 3 class | 3 class | 3 class |
| Normal force, [kN]                          | $N_{Ed}$      | 45.69    | 43.62    | 41.66   | 37.22   | 30.63   |
| Bending moment, [kNm]                       | $M_{Ed}$      | 102.8    | 84.28    | 67.45   | 52.24   | 38.61   |
| $N_{Ed}/A + M_{Ed}/W_{el}$ , [MPa]          |               | 36.72    | 33.92    | 30.80   | 27.24   | 80.89   |
| $f_y/\gamma_{M1}$ , [MPa]                   |               | 308.70   | 308.70   | 308.70  | 308.70  | 308.70  |
| Cross-section effort, [%]                   |               | 11.9%    | 11.0%    | 10.0%   | 8.8%    | 26.2%   |



The distribution of stresses reduced according to the Huber hypothesis was checked at the point where the cross-section suddenly changes (Fig. 2) and by the openings (Fig. 3); the distribution was then compared with the yield strength of steel.

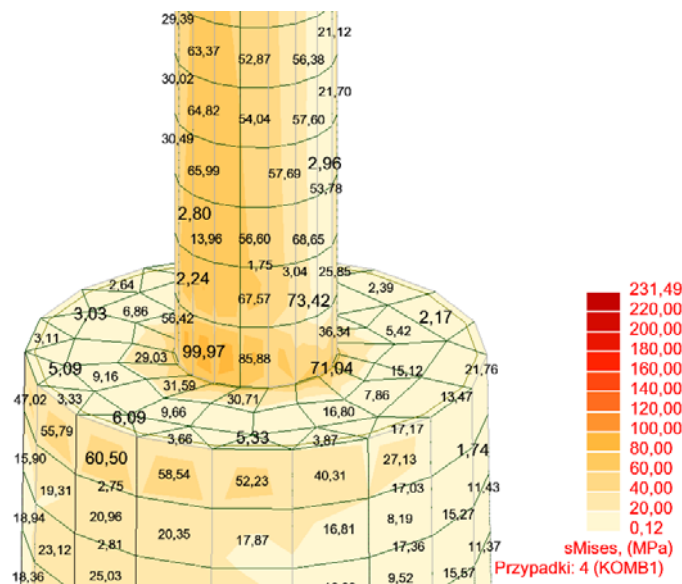


Fig. 2. Distribution of stresses reduced according to the Huber hypothesis at the point where the cross-section suddenly changes



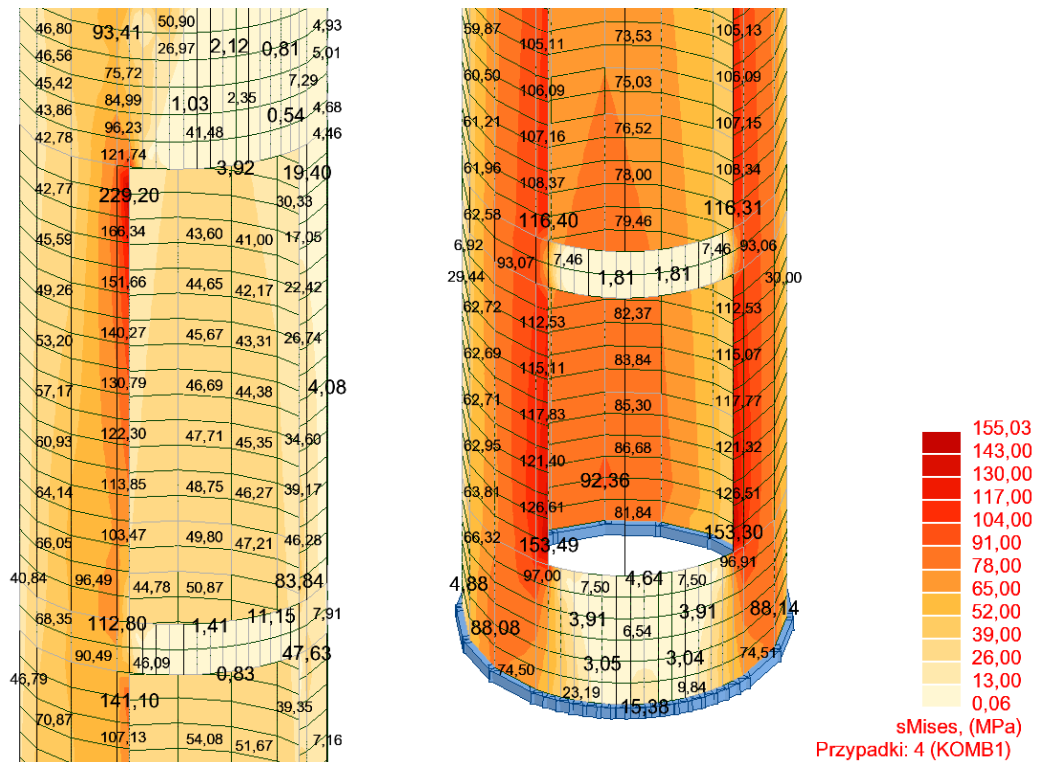


Fig. 3. Distribution of stresses reduced according to the Huber hypothesis by the openings

#### 4. FATIGUE ANALYSIS

Nominal, modified nominal or geometric stress ranges due to frequent loads  $\psi_I Q_k$  should not exceed the following values:

$$\Delta\sigma \leq 1.5 \cdot f_y, \quad (4.1)$$

where  $\psi_I = 0.2$  for wind actions.

It also should be demonstrated that for fatigue loading the following load-carrying capacity conditions are satisfied:

$$\frac{\gamma_{Ff} \cdot \Delta\sigma_{E,2}}{\Delta\sigma_c / \gamma_{Mf}} \leq 1.0. \quad (4.2)$$

where  $\gamma_{Ff}$  is partial factor for equivalent constant-amplitude stress ranges,  $\gamma_{Ff} = 1.0$  (according to PN-EN 1993-3-1),  $\gamma_{Mf}$  is partial factor for fatigue strength, taken as  $\gamma_{Mf} = 1.15$  for low consequence of failure of a structure assessed using the safe-life method,  $\Delta\sigma_c$  is the reference value of the fatigue strength at  $N = 2$  million cycles,  $\Delta\sigma_{E,2}$  refers to equivalent constant-amplitude stress range related to 2 million cycles, according to the relation:

$$\Delta\sigma_{E,2} = \lambda \cdot \Delta\sigma_E. \quad (4.3)$$

$\Delta\sigma_E$  is stress range related to  $N$  number of cycles,  $\lambda$  is equivalence factor given by the formula:

$$\lambda = \left( \frac{N}{2 \cdot 10^6} \right)^{\frac{1}{m}}, \quad (4.4)$$

where  $m$  is slope of the S-N curve for the case considered  $m = 5$ . For cantilevered structures, areas exposed to maximum fatigue stress ranges include the area of the joint with the foundation. For the structure considered, since the joint was reinforced by stiffening with lateral ribs, maximum stresses will occur in the cross-section above the ribs. The reference value of the fatigue strength for circular hollow sections is  $\Delta\sigma_c = 160.0$  MPa. For the least favorable case of fatigue loading (load directions are shown in Fig. 5), the equivalent stress range is equal to  $\Delta\sigma_{E,2} = 178.5$  MPa, so:

$$\frac{\gamma_{FF} \cdot \Delta\sigma_{E,2}}{\Delta\sigma_c / \gamma_{Mf}} = 1.28 > 1.0, \quad (4.5)$$

thus, the condition is not satisfied.

The solution is to design joint stiffening with larger lateral ribs. Figure 4 shows the differences in equivalent stresses without and with stiffening.

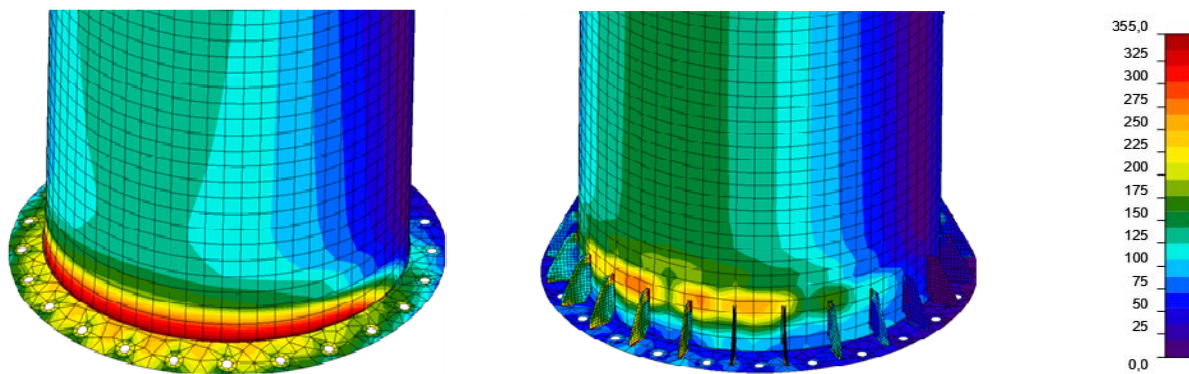


Fig. 4. Equivalent stresses in the tower base, stresses values in MPa.

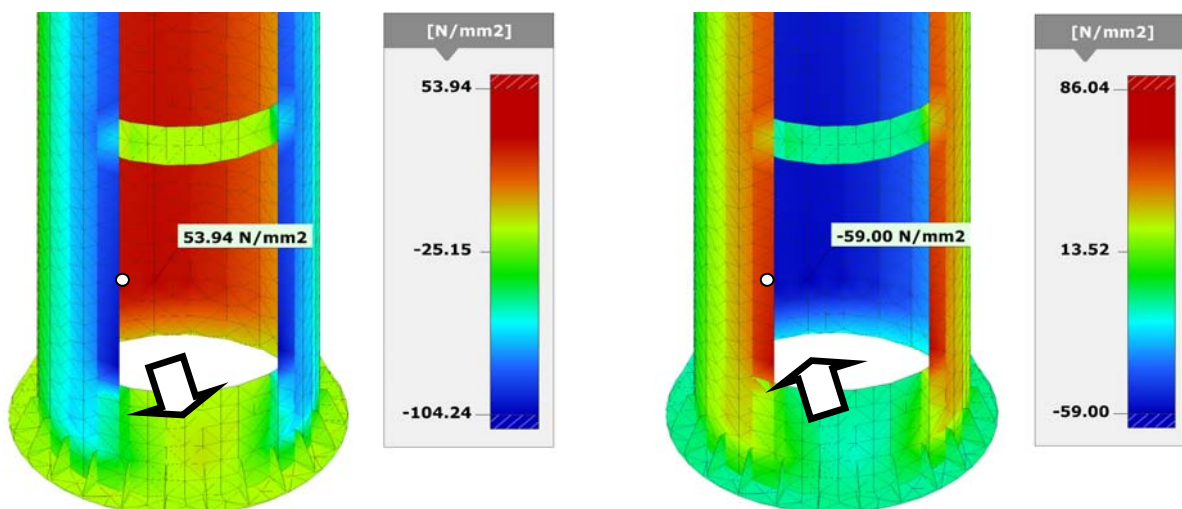


Fig. 5. Stress pattern at the joint with the foundation

#### 4. RESULTS AND CONCLUSIONS

Based on the analyses, the following conclusions can be drawn:

- The analyses indicated that the structural fatigue resulting from potential vortex excitation is crucial for monopole tower structures. Special attention should be paid to the connection between the tower's core and base where high values of stress were observed.
- One aspect that must not be neglected when designing solid-wall structures is technical openings of various types which make the cross-section weaker and should be always accounted for in the structural analysis. In the analyzed structure there is a stress concentration in the vicinity of the opening in segment S-4, providing access to telecommunications equipment serving the base station. To reinforce the edges of the openings in order to reduce stresses, L-sections, welded along the whole length of the segment should be designed on the inner side of the circular hollow section along the edge.
- The load-carrying capacity with respect to fatigue is exceeded by about 30%. To keep the load-carrying capacity, larger stiffening ribs at the joint of the tower core and the foundation should be provided.
- In order to reduce lateral vibrations of the structure caused by vortex excitation, and thus to satisfy the condition of the load-carrying capacity of the structure with respect to fatigue, the system cover of the upper segment of the tower should be equipped with turbulence mixers to disturb the regularity of vortex shedding at the upper part of the structure.
- Vortex excitation will occur only if the system beautification cover is mounted on the upper segment of the tower with antennas and equipment. If the telecommunication equipment is left without the cover, lateral vibrations will not occur and thus all the conditions of the load-carrying capacity of the structure will be met. It should be noted, however, that in this case wind actions on the tower core and the effort of each segment and joint would increase and the aesthetic qualities of the structure would deteriorate.

#### REFERENCES

- Smith, B.W. 2007. *Communication Structures*. Thomas Telford.
- Socket, H. 1994. *Wind-excited vibration of structures*. Wien: Springer-Verlag.
- PN-EN 1991-1-4: 2005. Eurocode 1 – Part 1-4: General actions. Wind actions.
- PN-EN 1993-3-1. Eurocode 3 – Design of steel structures – Part 3-1: Towers, masts and chimneys – Towers and masts.
- PN-EN 50341-1. Overhead electrical lines exceeding AC 1 kV — Part 1: General requirements – Common specifications.